Studies of RF discharge plasma behavior in the Uragan-3M and Uragan-2M torsatrons

I.M. Pankratov, A.A. Beletskii, V.L. Berezhnyj, P.Ya. Burchenko, V.V. Chechkin, L.I. Grigor'eva, D. Hartmann[1], R. Koch[2], V.G. Konovalov, A.Ye. Kulaga, G.G. Lesnyakov, A.V. Lozin, A.I. Lyssoivan[2], S.M. Maznichenko, Yu.K. Mironov, V.Ye. Moiseenko, V.K. Pashnev, A.A. Petrushenya, A.V. Prokopenko, V.S. Romanov, A.N. Shapoval, A.F. Shtan', D.A. Sitnikov, A.I. Skibenko, A.S. Slavnyj, S.I. Solodovchenko, E.L. Sorokovoy, Ye.L. Sorokovoy, O.M. Shvets, Yu.S. Stadnik, I.K. Tarasov, V.I. Tereshin, S.A. Tsybenko, N.V. Zamanov, Ye.D. Volkov

Institute of Plasma Physics, NSC KIPT, Akademicheskaya St. 61108 Kharkov, Ukraine
[1]Max-Planck-Institut für Plasmaphysik, Wendelsteinstraße 1, D-17491 Greifswald
[2]Laboratory for Plasma Physics - ERM/KMS, Association EURATOM - BELGIAN STATE, Avenue de la Renaissance 30, 1000 Brussels – Belgium

In the Uragan-3M (U-3M) and Uragan-2M (U-2M) torsatrons possibilities and prospects of Alfven method utilization for wall conditioning, plasma production and heating are studied.

Uragan-3M

U-3M is an $l = 3$, $m = 9$ small size torsatron with the major radius R_0 = 1 m, average plasma radius $\overline{a} \approx 0.12$ m and toroidal magnetic field $B_\varphi = 0.72$ T. The whole magnetic system is enclosed into a large 5 m diameter vacuum chamber (Fig.1); an open natural helical divertor is realized. The rotational transform at the plasma boundary is $\iota(\overline{a})/2\pi \approx 0.3$ and magnetic well is 14%. The working gas (hydrogen) is admitted into the chamber continuously at the pressure of 10^{-6}- 10^{-4} Torr. The plasma is produced and heated by RF fields (frame type antenna) at the frequency 8.8 MHz ($\omega \lesssim \omega_{ci}$) in the multi-mode Alfvén resonance regime [1]. The RF power P fed in the antenna amounts 200 kW. With this, a two-temperature ion energy distribution with a suprathermal tail is formed [2,3] (Fig.2, $P/\overline{n}_e$ =300kW/10^{12} cm^{-3}); the hotter and suprathermal ions are named as "fast ions" (FI)). The amount of FI rises with RF power. The FI outflow to the divertor predominantly on the ion $\mathbf{B}\times\nabla B$ drift side, thus indicating a substantial effect on FI loss of their trapping into toroidal and helical non-uniformities of the magnetic field [3,4]. Under certain values of B_φ, ω and plasma density $\overline{n}_e$ the coupling resonance appears. During this resonance a burst of enhanced FI outflow to the divertor occurs. The FI loss drives transitions to H-like modes in the RF plasma discharge of U-3M. The H-mode is a promising confinement regime by forming the edge transport barrier in tokamaks and helical systems [5].

Fig.1. Uragan-3M.

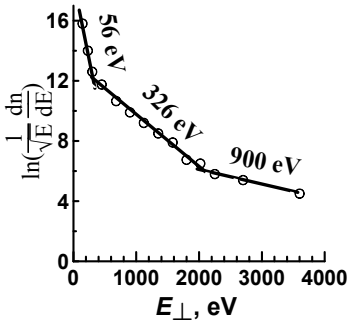

Fig.2. An example of CX neutral distribution in transversal energy.

Three phases of RF discharges in U-3M [6,7]. *First phase* (*Fig.3).* After discharge ignition, during the density $\bar{n}_e$ rise, the first burst-like outflow of fast ions to the divertor and an enhancement of high energy CX neutral flux Γ_n occur at $\bar{n}_e = \bar{n}_{e1} \approx 1.2\times10^{12}$ cm^{-3} independent of RF power. Beginning from some threshold power $P \approx 170$ kW, a regime with reduced level of edge potential fluctuation arises. The density continues to rise till t = 7.5 ms where a hard potential bifurcation to a higher value is distinctly observed at $\bar{n}_e = \bar{n}_{e3}$ ("first bifurcation"). At the threshold power $\bar{n}_{e3}$ is close to $\bar{n}_{e1}$ and increases with further P increase (Fig.4).

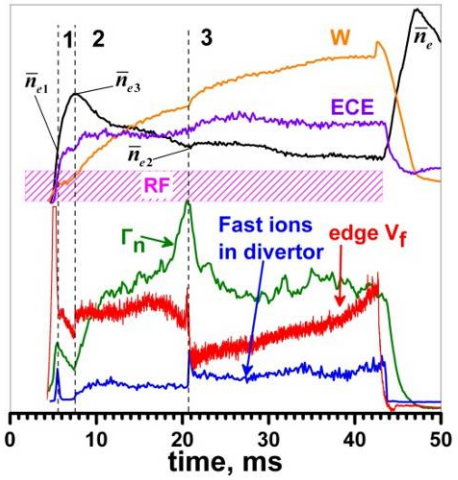

Fig.3. Three phases of discharge.

The second phase starts (Fig.3). After the bifurcation the plasma density decays and the fluctuation level is enhanced. In phase 2 the density decays up to $\bar{n}_e = \bar{n}_{e2} \approx 1.2\times10^{12}$ cm^{-3}, where a hard potential bifurcation to a lower value is observed ("second bifurcation").

Before this bifurcation, a short-time increase of the turbulent flux is observed. *Third phase (Fig.3).* At $\bar{n}_e = \bar{n}_{e2}$ the second burst of FI outflow to the divertor and an enhancement of high energy CX neutral flux Γ_n occur. The signals of diamagnetic energy content W and ECE (2nd harmonic) increase, while the edge turbulent flux drops (Figs.3, 5). The radial profile measurements of the edge floating potential V_f show strong change of the radial electric field gradient near the plasma boundary when going from phase 1 to phase 2 and from phase 2 to phase 3 (Fig.6). The suppression of turbulent flux near the rational magnetic surface $\iota/2\pi$ = ¼ inside the U-3M plasma, changes of the density and electron temperature profiles also are caused by the strong E_r shear formation [8].

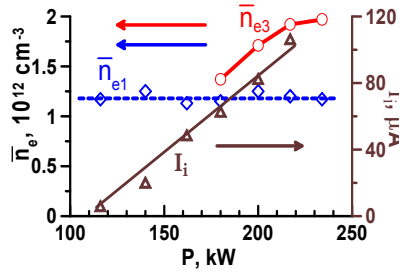

Fig.4. Values of $\bar{n}_{e1}$, $\bar{n}_{e3}$ and amplitude (I_i) of FI burst to the divertor, versus P.

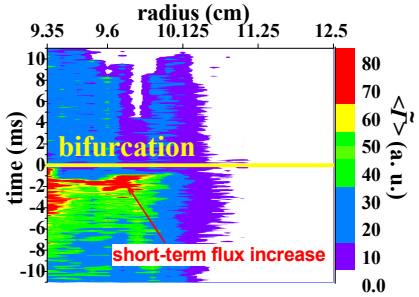

Fig.5. Space and time behavior of the turbulent particle flux.

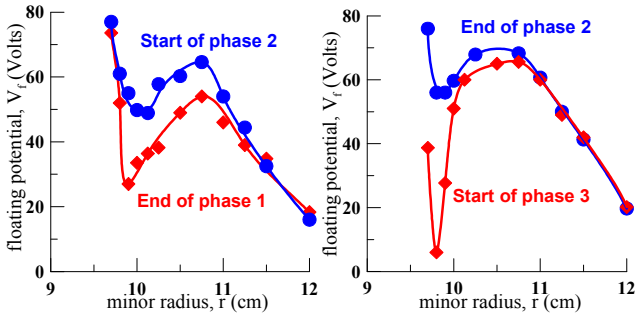

Fig.6. Radial profiles of V_f.

Conclusions. In U-3M, beginning from some threshold power $P \approx 170$ kW, the time behavior of RF discharge can be divided into three phases. As a result of the burst of FI outflow, the radial electric field changes [9]. A higher E_r shear (and a higher **E**×**B** velocity shear) at the phases 1 and 3 results in suppression of the edge turbulence and anomalous transport. H-mode-like regimes exist in phases 1 and 3. In phase 2 the L-like mode is observed. The next changes of ∇E_r are estimated from Fig.6: -520 V/cm^2 → -219 V/cm^2 (1→2) and -490 V/cm^2 → -1820 V/cm^2 (2→3).

Uragan-2M

U-2M is a medium size $l = 2$, $m = 4$ torsatron-type system with a small pitch angle of helical windings and additional toroidal field coils (R_0 = 1.7 m, $\bar{a} \approx 0.2$ m). The ultimate value of toroidal magnetic field is 2.4 T. Closed magnetic surfaces were measured for different values of toroidal and vertical fields. These measurements are in good agreement with calculated ones. The magnetic configurations with rotational transform $\iota(\bar{a})/2\pi > 1/3$ in the region near the magnetic axis and with $\iota(\bar{a})/2\pi < 1/2$ for outer surfaces are of practical interest. The magnetic well is 4.3%. At present toroidal magnetic field does not exceed B_φ = 0.6 T. U-2M is equipped with two compact RF frame antennas.

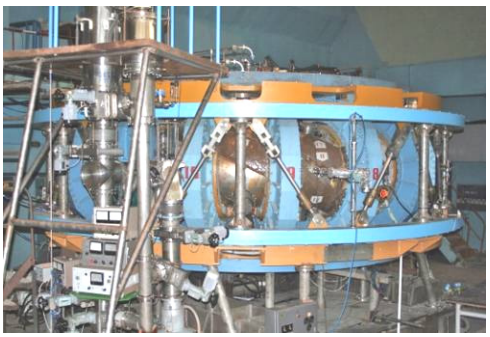

Fig.7. Uragan-2M.

The first antenna has a broad $k_{||}$ spectrum and is used for plasma production. The second one with narrower $k_{||}$ spectrum heats plasma in the Alfvén range of frequencies. Two generators with RF power 0.5 MW and frequency in the range of 10 MHz are used.

The antenna with the broad $k_{||}$ spectrum provides reliable gas break-down in the pressure range of (3×10^{-6} - 8×10^{-5}) Torr and produces plasma with the density $(1\text{-}2)\times10^{12}$ cm^{-3}. Combined use of two antennas with RF power P~100 kW (after preliminary short time wall conditioning) results in increase of the plasma density up to 6×10^{12} cm^{-3}. The increase of the carbon line intensity with time indicates that to improve plasma parameters, a careful wall conditioning is needed.

Wall conditioning [10]. Studies of wall conditioning by hydrogen discharges have been carried out. The cleaning is associated with the chemical reactivity of the atomic hydrogen capable to create volatile substances. The goal of such conditioning is removal of adsorbed species from the wall so that afterwards they can be pumped out of the vacuum chamber. The cleaning agents are the hydrogen atoms with Franck-Condon energies (about 3 eV) arising from dissociation of hydrogen molecules. If the electron temperature in the discharge was less than the ionization threshold, T_e= 4 -10eV, the dissociation rate was higher than the ionization one.

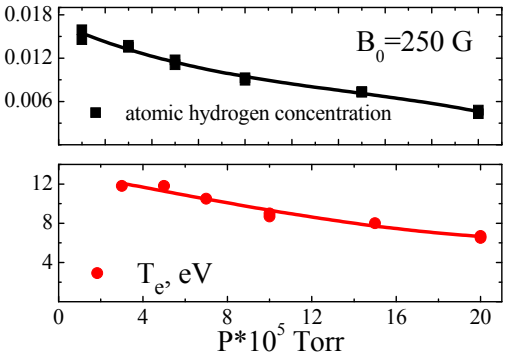

Fig.8. Dependence of atomic hydrogen concentration and electron temperature on hydrogen pressure.

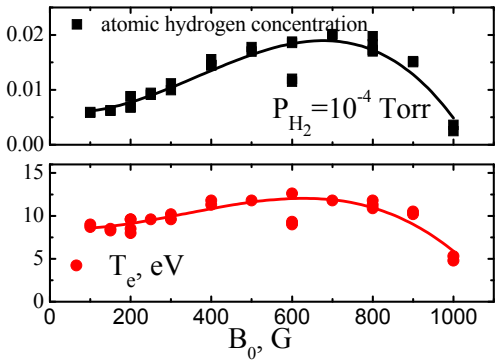

Fig.9. Dependence of atomic hydrogen concentration and electron temperature on axial magnetic field.

A double frame antenna was used for wall conditioning. Continuous RF discharges are sustained by the 1 kW RF oscillator in the frequency range 4.5-8.8 MHz. Such a small power creates a plasma with low density up to $n_e = 8\times10^9$ cm^{-3}. The measurements are performed by the optical diagnostics, Langmuir probes and microwaves. Before and after discharges a mass

spectrometry is used to analyze the residual gas composition. Because of the electron temperature is low, T_e<20eV, T_e is calculated following [11] from the integral emission of Fulcher-α series to H_α line intensities ratio. The concentration of neutral hydrogen atoms $C_H = n_H / n_{H2}$ is calculated from the analysis of the intensities of spectral lines of Balmer series [12]. The key moment here is the separation of the emission induced by the excited atoms and the emission resulted from the dissociative excitation of molecules.

The discharge fills up the whole plasma column and follows the stellarator magnetic configuration. The dependences of the electron temperature and of the neutral atom concentration calculated from the optical measurements are shown versus neutral gas pressure in Fig. 8 and versus magnetic field on axis in Fig. 9. The decrease of the temperature with rising pressure is higher than expected. The dependences demonstrate that the discharge could be sustained in very wide range of discharge conditions. As it is seen from Fig. 9, the optimum magnetic field is B_{0opt} = 600 G, however, in reality a lower magnetic field for B_0 = 250 G is chosen for wall conditioning.

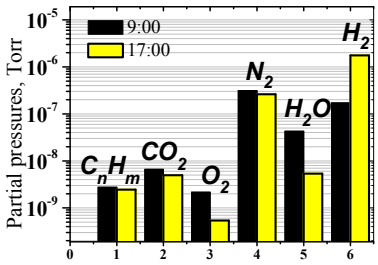

Fig.10. Mass-spectrometer measurements of partial pressures before and after 6-hour RF discharge.

The wall conditioning is controlled by the behavior of mass composition of the residual gas. The evolution of the gas components within a single operation day (see Fig. 10) indicates a removal of oxygen and water and a slow removal rate for hydrocarbons.

The continuous discharge is also combined with a 50-100 kW, 5.6 MHz pulse discharge, with the pulse length being 10-20 ms and the repetition rate being 2-5 pulses per minute. In the combined discharge the time of wall conditioning shortens. Both discharges seem to be suitable for wall conditioning and have a prospect for use in superconducting devices.

A new four strap compact antenna [13]. The prior theoretical studies had shown the possibility to use the wave with high $k_{||}$ for Alfvén resonance heating [14]. Here a compact multi-strap antenna which size is similar to that of the ICRH antennas can be used [15]. In this way the major deficiency of the Alfvén resonance heating is avoided.

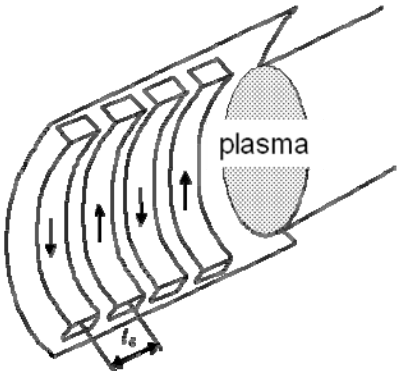

Fig.11. The strap width is 10 cm and the distance between the central lines of neighboring straps equals 20 cm. The poloidal strap length is 40 cm, $<k_{||}> \approx 0.17\ cm^{-1}$.

The mode conversion scheme with a high value of $k_{||}$ will be used in U-2M for RF production and heating a plasma with density up to 1.6×10^{13} cm^{-3} with using a new four-strap compact antenna (Fig. 11). The Alfvén resonance heating is examined numerically in the approximation of radially non-uniform plasma cylinder with identical ends. The numerical model for wave excitation and propagation accounts for the longitudinal electron thermal motion and the finite ion gyroradius. This model allows to treat correctly the propagation and damping of the kinetic Alfvén wave in hot plasmas. With this antenna the periphery plasma heating is suppressed and there is no sensitive dependence on the plasma parameters. The same antenna could be used for ICRH.

The schematic picture of Alfvén resonance heating is sketched in Fig. 12. The wave field excited by the antenna penetrates the plasma through the cut-off layer. This layer extends from the plasma boundary to a radial position that is not much nearer to the antenna than

the Alfvén resonance location. Then in the vicinity of the Alfvén resonance the wave conversion occurs and the slow wave is generated. In warm plasma it travels towards the plasma density maximum. In cold plasma it propagates to the plasma edge.

In general, the antenna generates waves with all poloidal and toroidal mode numbers. Thus,

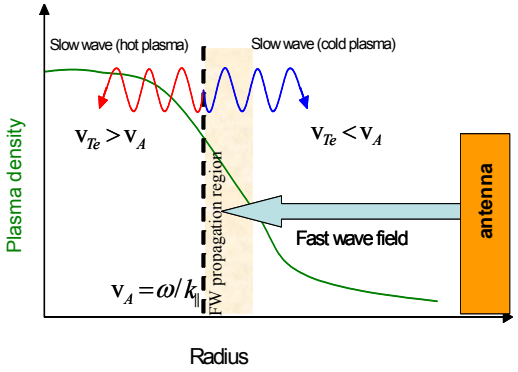

Fig.12.Scheme of Alfvén resonance heating.

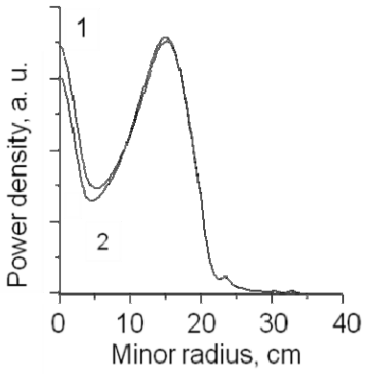

Fig.13.Power deposition profile. Landau damping and ion cyclotron wave damping (the fundamental cyclotron harmonic) are taken into account; parabolic profiles: $T_e(0)=500eV$ and $T_i=0$ (curve 1); $T_e(0)=500eV$ and $T_i(0)=200eV$ (curve 2). B_0= 0.5 T, $n(0)=8\times10^{12}$ cm^{-3}, $\omega=0.82\omega_{ci}$, $\omega=4.2\times10^{7}$ c^{-1}

a number of Alfvén resonances are excited. Many of them are located at the plasma periphery. There the Alfvén velocity is high and electron thermal velocity is low. The converted slow wave is locked at the plasma periphery and heats the scrape-off-layer plasma. This results in a waste of RF power and stimulates impurity production. So, the suppression of low $k_\parallel$ wave field generation by the antenna should be provided. Fig. 13 displays profiles of the power deposition for two values of ion temperature. The antenna provides power deposition outside the plasma column, but it is reasonably small. The major power deposition is at r = 15 cm, but some energy reaches plasma column center. The slow wave propagates to the plasma column center and the central increase of the power deposition is owing to the wave focusing. The curves corresponding to different ion temperatures have small distinctions in the plasma core only, where the ion temperature takes a maximum value. Hence, the influence of finite Larmor radius is small.

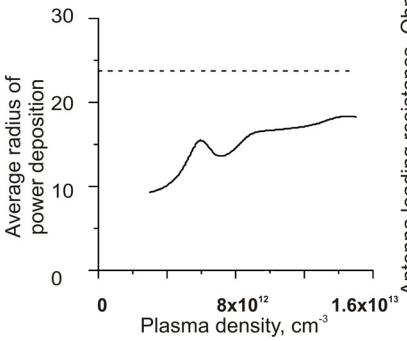

Fig.14. The average radius of power deposition versus of plasma density.

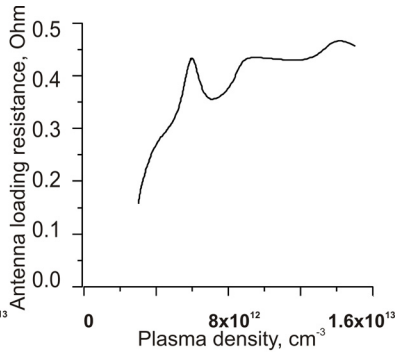

Fig.15. The density dependence of antenna loading resistance.

The quality of heating is characterized by the dependence of average radius of power deposition, $< r >= \int P_{RF} r dV \Big/ \int P_{RF} dV$, on plasma density (Fig.14). Fig. 15 shows the density dependence of antenna loading resistance per strap.

Conclusions. The increase of the carbon line intensity during the first RF plasma production in U-2M indicates that a careful wall conditioning is needed for improving the plasma parameters. Physical features of the low-power RF discharges producing hydrogen atoms are studied in a very wide range of the neutral gas pressures and magnetic field values. The continuous discharge and continuous discharge combined with a pulse discharge are investigated

for wall conditioning. Both discharges look to be suitable for wall conditioning and, after certain improvements, have a prospect for use in superconducting machines.

A compact four-strap antenna is proposed for Alfvén resonance heating in U-2M. For this antenna periphery plasma heating is suppressed, both low and high density plasma heating are possible. There is no sensitive dependence on the plasma parameters.

Acknowledgements

The studies of Uragan-2M were partly performed within the frame of the STCU Project No.4216.

References

1. Shvets O. M., Dikij I. A., Kalinichenko S. S. et al. Nucl. Fusion **26** (1986) 23.
2. Volkov E. D., Adamov I. Yu., Arsen'ev A. V. et al. Proc. 14th IAEA Conf. on Plasma Physics and Controlled Nuclear Fusion Research (Würzburg, Germany, 1992) Vienna: IAEA, 1993. Vol. 2, p. 95.
3. Chechkin V. V., Grigor'eva L. I., Sorokovoy E. L. et al. Nucl. Fusion **43** (2003) 1175.
4. Chechkin V. V., Grigor'eva L. I., Smirnova M. S. et al. Nucl. Fusion **42** (2002) 92.
5. Wagner F., Hirsh M., Hartfuss H.-J. et al. Plasma Phys. Control. Fusion **48** (2006) A217.
6. Chechkin V.V., Grigor'eva L.I., Sorokovoy Ye.L. et al. Plasma Phys. Reports **35 (**2009) 852.
7. Beletskii A.A., Grigor'eva L.I., Sorokovoy E.L. et al. Plasma Phys. Reports **35 (**2009) 818.
8. Volkov E. D., Berezhnyj V. L., Bondarenko V. N. et al. Czekh. J. Phys. **53** (2003) 887.
9. Shaing K. C., Crume E. C., Jr. Phys. Rev. Lett. **63** (1989) 2369.
10. Moiseenko V.E., Burchenko P.A., Chechkin V.V. et al. Wall Conditioning RF Discharges in Uragan-2M Torsatron, 36th EPS Conference on Plasma Physics (2009, Sofia, Bulgaria) P5.199.
11. Kondo K., Okazaki K., Oyama H., et al. Japanese Journ. of Applied Phys. **27** (1988) 1560.
12. Fujimoto T., Sawada K., Takahata K. J. Appl. Phys. **66** (1989) 2315.
13. Moiseenko V.E., Volkov Ye. D., Tereshin V. I., Stadnik Plasma Phys. Reports **35 (**2009) **(**in press)**.**
14. Puri S. Nucl. Fusion **27** (1987) 227.
15. Moiseenko V.E. "Alfvén Heating in Toroidal Plasmas by Using Three-Half- turn Loop Antenna" in IAEA TCM (Proc. 8th Int.Workshop on Stellarators, Kharkov 1991), IAEA, Vienna (1991) 207.